*Kaleem, Saqib; Humbla, Stefan; Müller, Jens; Rentsch, Sven; Stöpel, Dirk; Hein, Matthias:*

# Reconfigurable 4 × 4 switch matrix for Ka-band Geo-stationary satellite mission

***URN:*** urn:nbn:de:gbv:ilm1-2015210230

*Published OpenAccess:* January 2015

*Original published in:*

Frequenz : journal of RF-engineering and telecommunications. - Berlin : De Gruyter (ISSN 2191-6349). - 66 (2012) 11/12, S. 347-357.
*DOI:* 10.1515/freq-2012-0105
*URL:* http://dx.doi.org/10.1515/freq-2012-0105
*[Visited:* 2015-01-14]

DOI 10.1515/freq-2012-0105 — Frequenz 2012; 66(11-12): 347–354

Saqib Kaleem*, Stefan Humbla, Jens Müller, Sven Rentsch, Dirk Stöpel, and Matthias Hein

# Reconfigurable 4 × 4 Switch Matrix for Ka-Band Geo-Stationary Satellite Mission

**Abstract:** A 4 × 4 reconfigurable switch matrix based on low temperature co-fired ceramic technology for Geo-stationary satellite mission at Ka-band downlink frequencies (17–22 GHz) is presented. In comparison to its predecessor, the new generation of switch-matrix features augmented functionality whilst an overall reduced size (40%). The distinguished characteristics include the shifting of matching networks from top-layer into the embedded layers of the multilayer ceramic stack and the elimination of two external peripherals required to digitally control the bipolar current sources of the PIN-diodes based switch integrated circuits. As an additional functionality, four passive transparent paths between corresponding input and output are integrated within the module, to exhibit rudimentary transmission through the module in case of on-board power failure.

**Keywords:** low temperature co-fired ceramics (LTCC), reconfigurable switch matrix, shielded coplanar waveguide, Ka-band geostationary satellite

**PACS® (2010).** 77, 73, 84, 85, 89

***Corresponding author: Saqib Kaleem:** Institute for Micro- and Nano-Technologies, Ilmenau University of Technology, Ilmenau, 98693 Germany, E-mail: saqib.kaleem@tu-ilmenau.de
**Stefan Humbla:** Institute for Micro- and Nano-Technologies, Ilmenau University of Technology, Ilmenau, 98693 Germany.
**Jens Müller:** Institute for Micro- and Nano-Technologies, Ilmenau University of Technology, Ilmenau, 98693 Germany.
**Sven Rentsch:** Institute for Micro- and Nano-Technologies, Ilmenau University of Technology, Ilmenau, 98693 Germany.
**Dirk Stöpel:** Institute for Micro- and Nano-Technologies, Ilmenau University of Technology, Ilmenau, 98693 Germany.
**Matthias Hein:** Institute for Micro- and Nano-Technologies, Ilmenau University of Technology, Ilmenau, 98693 Germany.

## 1 Introduction

The low temperature co-fired ceramic (LTCC) technology offers a cost-effective solution for multilayer hybrid integrated-circuits (ICs) [1]. Technological advancements have enabled sophisticated LTCC modules, consisting of microelectronics, cooling or heating systems, sensors and actuators, and microsystems, compressed in a single package [2], [3]. The electrical and mechanical properties, high-reliability and stability of three-dimensional (3D) microstructures have established the LTCC technology for wireless, automotive, military and space applications [4].

During the course of research projects [5] and [6], several functional modules i.e. transceivers, synthesizers and reconfigurable switch matrix (RSM) have been developed and combined in different experiments, with the aim to verify the KERAMIS® technology [7] for space applications and space-qualification of individual modules. Consequently, the LTCC based RSM module has undergone subsequent modifications resulting in three generations, shown in Fig. 1. The Generation-II (2G) of the RSM module has successfully passed space-qualification stages and set the design constraints (in terms of mass, surface area as well as electrical characteristics and mechanical robustness) for later generations. The 2G is one of the modules aboard the German test satellite TET-1 (Technology Evaluation Carrier), designed for the purpose of one-year On-

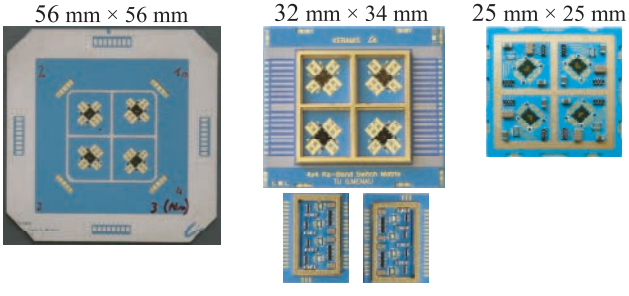


**Fig. 1:** The chronological evolution of the LTCC based RSM module from left to right. Generation-I (left) without bias-circuitry is developed for functional verification, 2G (center) with two external bias peripherals, 3G (right) with integrated biasing circuitry.

This work was supported by the German Federal Ministry of Economics and Technology (BMWi) under the project management by the German Aerospace Center (DLR, no. 50YB1112).

Orbit-Verification (OOV) [8]. TET-1 has successfully been launched into orbit on 22nd July 2012, providing a test-bed to observe the correct in-orbit operation and reliability of 2G RSM [9]. This paper presents the recent modifications of the 2G version, resulting in a newer generation (3G). The 3G version is a compact module with denser integration of functional components whilst overall reduced size compared to its predecessor. The surface area of 3G measures 25 mm × 25 mm, compared to 32 mm × 34 mm of 2G version, providing a 40% reduction in size with similar functionality. In addition, the biasing circuitry required for PIN-diodes is integrated on the vacant surface of the 3G module, thereby eliminating two external peripherals from the carrier board.

In the recent evolution of the RSM, 3G version is required to be adapted for upcoming German Geostationary satellite mission, H2Sat (Heinrich-Hertz) [10]. The order of the operational life-time of geostationary satellites (15 years or more) necessitates high reliability of its individual constituents. Additional redundant modules are required to ensure full, reduced, or minimum functionality in case of malfunction. A rudimentary function in case of on-board power-failure i.e. to bypass the RSM module and to establish a transparent path between corresponding inputs and outputs, guarantees a transmission through the module. This paper presents a passive solution for the implementation of the transparent paths within the RSM module. A schematic representation of the modified 3G module (named as 4G) required for H2Sat is shown in Fig. 2.

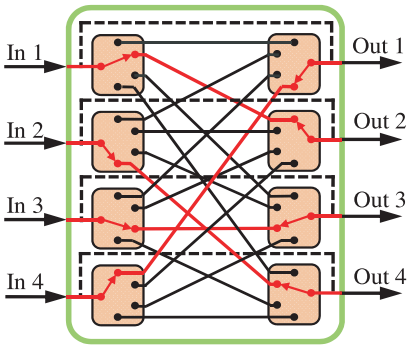


**Fig. 2:** Functional view of the 4 × 4 microwave switch matrix, required for the H2Sat mission, using eight SP4T switches. A possible switch configuration is depicted in red (electrically active paths), while black lines represent the isolated paths, in normal operation. The dotted lines are active only in power-fail condition.

## 2 4 × 4 3G Reconfigurable switch matrix

Common to the three generations of the RSM module, eight SP4T switch-ICs (MACOM MA4SW410B-1) are mounted using double-side hybrid integration, resulting in compact lateral dimensions. The switch-ICs are placed symmetrically in cavities on the top and bottom of the multilayer LTCC substrate (DuPont 951 Green Tape™ thick-film system), as shown in Fig. 3. Despite possessing reasonable dielectric microwave losses compared to low-loss tapes, the system is chosen because of its reliable manufacturability, wide range of available pastes, and its hermetic packaging capabilities fulfilling the requirements in terms of reliability. The eight-layer stack of the RSM utilizes DuPont 951 PX substrates, exhibiting sintered heights of 213 µm each. The symmetrical stacking results in a unified warp-less package after the sintering process.

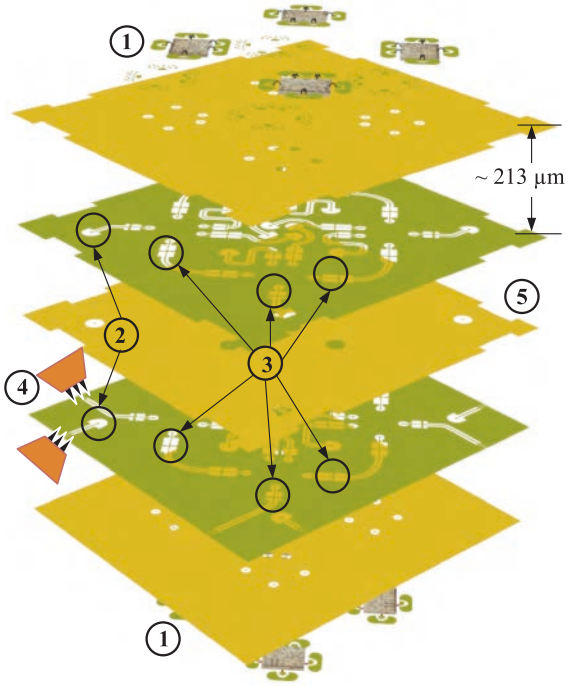


**Fig. 3:** Exploded view of the 3D-layout of the 3G RSM depicting constituent passives i.e. double-side mounted switch-ICs (1), vertical transitions (2), matching networks (3), wafer-probe contact-pads (4) and 5-layer cavities (5) in the exterior to shorten the second-level interconnects to the carrier board. DC paths at layer-2 and layer-7 as well as the ground-vias between layers are omitted for clarity.

The switch-ICs are interconnected via matching networks. In contrast to the 2G version, the matching networks are shifted from surface layers into buried layers. In consequence of the permittivity change of the surrounding dielectric, a radical re-adjustment of the matching net-

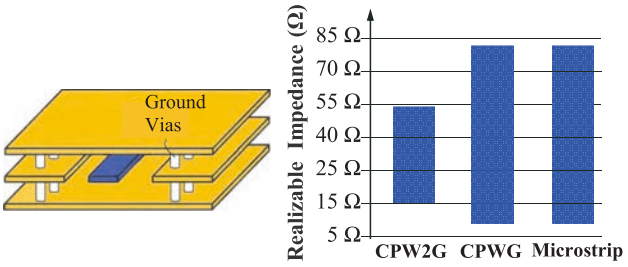


**Fig. 4:** Two-sided vertically shielded coplanar waveguide (CPW2G) configuration [10] and the range of realizable characteristic impedance of different transmission media within the technological constraints (line-widths and gaps ≥ 70 µm) for $\varepsilon_r \approx 7.6$.

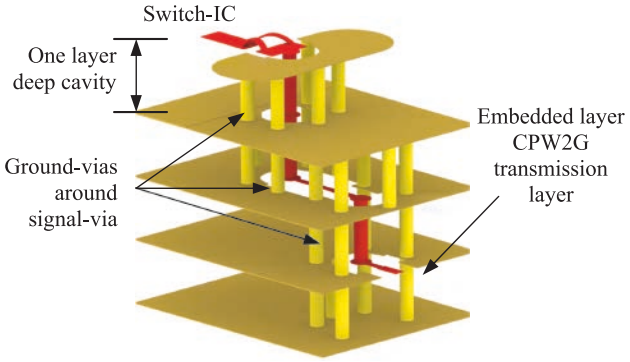


**Fig. 5:** First-level interconnect with two 60 µm × 20 µm bond-ribbons, each 450 µm long and with an angular displacement of ~34° between them.

works with simultaneous consideration of technological constraints (minimum line-widths and gaps ≥ 70 µm) was mandatory.

The embedded layer passive structures are realized using a variant of coplanar waveguides (CPW), shielded by vertical ground planes on both top and bottom sides (CPW2G) [11]. This type of waveguide, due to homogenous surrounding media, exhibits low radiation, low dispersion, and high isolation over a broad range of frequencies and is therefore utilized for embedded passive structures within the RSM module. Among the shortcomings of this particular configuration is the limited range of realizable characteristic impedance [12]. The characteristic impedance of transmission lines depends on frequency, dielectric permittivity, geometry and the propagating mode. Within the technological constraints, a comparison of realizable impedance using CPW2G transmission lines (15–25 Ω) with the microstrip and grounded-coplanar-waveguide (12–83 Ω) is shown in Fig. 4.

The shifting of matching networks to buried layers emancipates the area on both top and bottom surface layers, which is then utilized to integrate the digitally controlled bipolar current sources and associated passives, required to bias the switch-ICs, eliminating two external peripheral modules (present in 2G). In the following, constituent functional components of 3G RSM module are detailed.

## 2.1 First-level interconnect and interlayer vertical transition

The monolithic microwave integrated circuits (MMIC) are connected to the passive circuit elements on the ceramic substrate by first-level interconnects. Besides impedance discontinuity, first-level interconnects introduce parasitic inductance, and are therefore detrimental to the overall system performance. Two parallel gold-ribbons with a cross-section of 60 µm × 20 µm are used as first-level interconnect between the SP4T switch-ICs and the LTCC package. This configuration, whilst within manufacturing limits, provides smooth impedance and mode transition [12]. The 3D electromagnetic simulation model is depicted in Fig. 5. The dimensions and, thereby, the impedance of the bond-pads are adjusted to yield low reflection and low insertion loss across the Ka-band downlink frequency range (17. . .22 GHz).

The RSM module consists of three different vertical inter-layer transitions. The first transition, adjacent to the bond-pad of the first-level interconnect, is a three-layer transition from a grounded coplanar waveguide (quasi-TEM mode) to a vertically shielded coplanar waveguide (TEM mode). The other two vertical transitions are between the two CPW2G waveguides and are only two layers high. Unlike [13], these transitions are completely shielded from the top and bottom ground-layer metallization, assisting in routing DC paths through the inner layers. Therefore, these transitions preserve the propagation of TEM modes at the two ends. While one internal transition is straight (0°), the other one provides a 180° turn. Again in distinction from [13], the 180° transition is realized using 0°-transition with a lateral 180°-turn. This approach yields broadband characteristics, however, at the expense of increased transmission loss.

Common to the three vertical transitions, the coaxial-via scheme is utilized [14], [15]. Based on the concept of impedance matching, transitions exhibiting low reflections ($S_{11} \leq -25$ dB) are designed, under the technological constraints of KERAMIS® technology, i.e. the minimum signal-via diameter of 150 µm and catch-pads of 200 µm. The resulting vertical coax-like waveguide has large cross-section. Openings are introduced in the ground planes immediately above and below the signal-vias to raise the

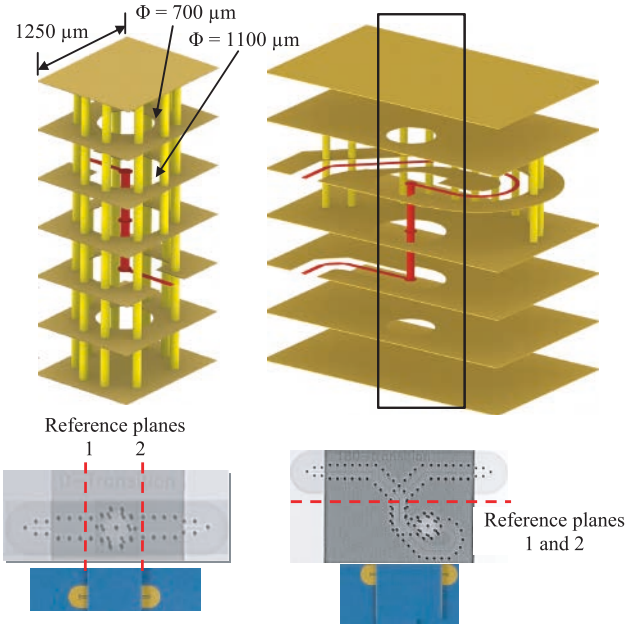


**Fig. 6:** Inter-layer vertical transitions, 3D EM – simulation models for the 0°-transition and 180°-transition (top), manufactured prototype substrates and X-ray images show the shifted reference planes for extracting scattering parameters of transitions.

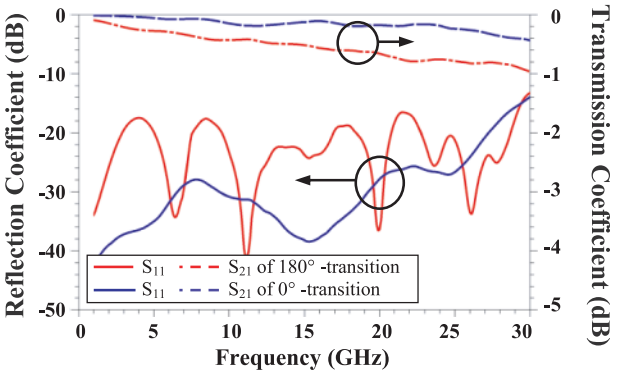


**Fig. 7:** Extracted scattering parameters of 0°- and 180°-transitions at the reference planes marked in Fig. 6.

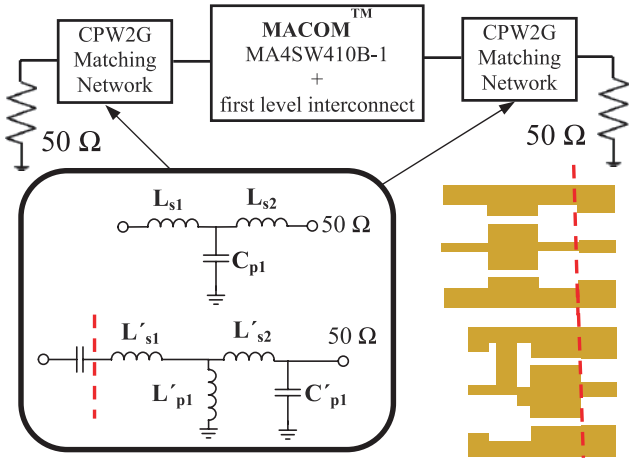


**Fig. 8:** Simulation model for the design of the bilateral matching networks in the CPW2G waveguides (top), equivalent lumped-element and distributed models for the stepped-impedance and Levy matching networks developed during two design iterations of the 3G RSM (bottom).

impedance and to broaden the bandwidth of the transitions with reduced lateral-dimensions. Various design parameters are adjusted to limit the lateral dimensions of the transitions within 1300 µm. Miniaturized transitions enable close arrangement of switch-ICs and thereby minimize lateral dimensions of the module.

The 3D electromagnetic simulation models of the transitions and the ceramic structures manufactured for on-wafer measurements are shown in Fig. 6. X-ray images of the inner layers visualize the reference planes. The S-parameters were extracted from 1 GHz to 40 GHz using the two-tier multiline TRL calibration procedure [16], [17]. The extracted S-parameters, in Fig. 7, show broadband matching characteristics. The transmission loss of the 180°-transition is large compared to the 0°-transition. The difference is associated with the significant variation in line-widths/gaps of the transmission line bend around the signal-via transition.

## 2.2 Matching network

The fundamental component of the RSM is a single-pole-four-throw (SP4T) switch-IC (MACOM M/A4SW410B-1). During an earlier characterization step, the scattering parameters of the switch-IC were measured together with the first-level interconnect. The measurement setup and the measured results were presented in [18]. To further improve the microwave performance in the frequency range of interest (17. . .22 GHz), matching networks were placed at each of the five microwave ports of the switch-IC. A block diagram representation for the bilateral design of the matching networks is shown in Fig. 8.

In the first design iteration, the buried-layer matching networks consisting of three-element stepped impedance connected in a low-pass T-network was designed and manufactured. A nomenclature of naming the various microwave and DC interfaces is shown in Fig. 9, where the port marked with '1o' represents the switch-IC in the first left-top quadrant while the one marked with '3u' is the switch-IC in the right-bottom quadrant. Therefore, a transmission path from top-left switch-IC to the right-bottom switch-IC is termed as 1o-3u, for instance. The 16 trans-

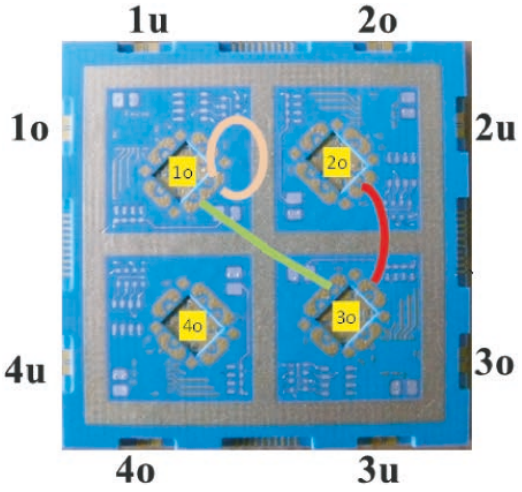


**Fig. 9:** Nomenclature for microwave and DC interfaces of the LTCC RSM. The three distinct groups of transmission paths in the embedded layers are color-marked. Uni-planar transmission paths (red), with 0°-transition (green) and with 180°-transition (orange).

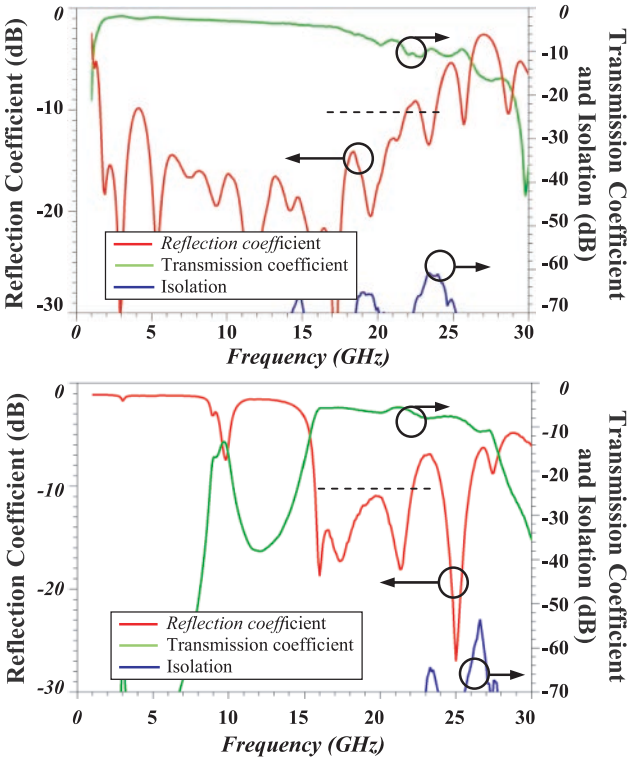


**Fig. 10:** Measured S-parameters of the 3G RSM – first design iteration using stepped impedance matching network (top), second design iteration using Levy matching network (bottom).

mission paths in the RSM can be split into three distinct groups; 8 uni-planar paths between adjacent switch-ICs, 4 paths between switch-ICs opposite to each other connected by a 0°-transition, and 4 paths between switch-ICs on top of each other connected by a 180°-vertical transition. The measured scattering parameters for transmission (forward bias the two SP4T switch-ICs i.e. 5 V, 10 mA) and isolation (reverse bias the two switch-ICs i.e. –10 V) of the transmission path 3o-1u are shown in Fig. 10. Broadband characteristics (reflection coefficient < –10 dB) up to 21 GHz was observed. The moderate reflection coefficient as well as the ripples in the transmission coefficient across the operational frequency range needed further improvement. Increased parasitic capacitance due to ground metallization and the limited value of the maximum realizable impedance of the CPW2G transmission lines restrict the achievable quality factor and shift the self-resonance frequency of the buried-layer distributed inductors to lower values. During later simulations and measurements, therefore, it was not possible to improve the scattering parameters with 3- or even 5-element stepped-impedance matching networks. An approach using air-cavity beneath the substrate can improve the situation [19]. However, additional cavities in the ceramic substrate have not been favored during space-qualification of earlier generations of RSM module and alternate configuration of matching network had to be developed in the later design iteration.

In the second iteration, a 2-element Levy matching network was designed, which is considered to be optimal matching network for a restricted class of RLC loads [20]. Starting from the lumped-element equivalent model of the switch-IC measurement at the center frequency (~19.5 GHz), a mathematical formulation yielded lumped-element equivalent model of the matching network. The lumped-element model of the matching network contained an impedance transformer which was replaced by the application of the Norton transformer equivalence, yielding additional lumped elements [21]. The resulting matching network and its distributed counterpart are shown in Fig. 8. The two benefits achieved using this type of network included the omission of the transmission lines with narrow widths (i.e. close to technological constraints) for the realization of high impedance lines and the presence of a short-circuited stub.

The RSM module is intended to serve a Geo-stationary satellite mission and therefore, it will be exposed to radiation from different sources during its operation [22]. Reliable operation of the RSM module over the lifetime of the satellite requires minimization of detrimental effects potentially caused by destructive radiation. Considering the matching network of the first iteration, high-energy ionized particles would accumulate on the signal path (bearing no return-paths, i.e. floating potential) between the switch-ICs. Thereby, regions of high-charge density

would exist on the ceramic substrate. In the second iteration, the short-circuited stub in the Levy matching network provided return path to the carrier-board (shorted microwave and DC grounds). Besides Kovar-shielding, the short-circuited stub aids to the robustness of the 3G RSM against radiation.

The measured scattering parameters of the transmission path 3o-1u with Levy matching networks are shown in Fig. 10. A band-pass characteristic in the Ka-band (17. . .22 GHz) is observed with an insertion-loss of $6 \pm 0.8$ dB, matching of –10 dB and isolation better than 70 dB.

### 2.3 Integration of PIN-diode drivers

Like the preceding version, the 3G RSM comprises 96 PIN-diodes requiring 32 bipolar currents. To provide digital control, a biasing circuitry is required to transform the digital TTL-levels to bipolar currents. The vacated area on surface layers creates the possibility to integrate bare-die diode-drivers and associated passives in the same module. The large number of DC signals enforces the routing of control signals in the inner layers (second layer from both top and bottom surfaces) of the module. The RSM will eventually be hermetically sealed by a Kovar lid (21 mm × 21 mm). The passives are mounted using glue and wedge-wedge bonding. This strategy avoids additional cavities on the substrate, resolving issues associated with the vibration tests during the challenging space-qualification process [23].

## 3 Power failure redundancy

In the event of an on-board power-failure, the redundant paths, shown in Fig. 2, link each input to the corresponding output. The implementation of redundant paths, therefore, requires only passive components for its realization. Relying on the reflective behavior of the switch-ICs in the power-fail state, a possible passive solution based on cascaded quadrature hybrid couplers is presented [18]. Cascaded couplers with continuously adjustable coupling ratio are presented in [24]. However, for this particular case, only two states are required for switching the signal paths which implies the use of switching elements like PIN-diodes.

The operational bandwidth requirement of over 25% enforces to use a two-section branch line coupler with optimal design values, such as suggested in [25]. In consequence of the limited range of realizable impedance values, design values are normalized with respect to low

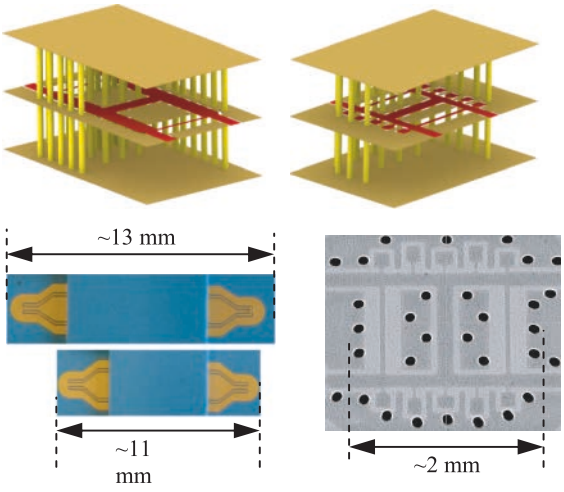


**Fig. 11:** 3D EM simulation models of buried-layer quadrature couplers – conventional (left-top), miniaturized (top-right), manufactured prototypes for dual-probe 4-port measurements (bottom-left) and X-ray images of the 50% miniaturized coupler (bottom-right).

impedance i.e. 28 Ω is performed. The resulting cascaded couplers structure exceeds 9 mm in lateral dimension. This dimension, however, is required to be reduced to sustain a compact size of the RSM module whilst remaining within the dimensional constraints for space qualification. A 50% size reduction is achieved by distributed capacitive-loading the coupled arms of the couplers [26]. The simulation model, manufactured ceramic substrate and the X-ray image of the embedded layer reduced-length coupler are shown in Fig. 11.

Appropriate matching networks, vertical transitions, terminations, blocking capacitors, and efficient distribution of four miniaturized couplers in the multilayer substrate are required to meet the dimensional constraint of space-qualification as well as the mounting requirements of the RSM module on the organic carrier-board.

## 4 Conclusions

A compact advanced generation (3G) of the reconfigurable switch matrix module based on Low Temperature Co-fired Ceramic technology for the Ka-band Geo-stationary satellite mission is described. By using embedded passive structures, the matching networks were shifted from the surface layers into buried layers, accommodating PIN-diode drivers within the RSM module, eliminating two external peripherals. The 3G module has a surface area of 25 mm × 25 mm, achieving an area-gain of 40% compared to its predecessor (2G). Optimal matching net-

works for the class of complex loads replaced the step-impedance matching networks in the second design iteration. The presence of short-circuited stub in the matching networks improves the robustness of 3G RSM module against radiation, besides shielding provided by a Kovar-lid.

To improve the availability of the payload in case of on-board power-failure, the RSM module is required to exhibit transparent characteristics between corresponding inputs and outputs. The paper presented a passive solution to exhibit redundant transmission path, capable to be incorporated within the LTCC module. The transparent paths bypass the core of the RSM module and are active only in power-fail case.

The experimental verification of the miniaturized quadrature coupler, the distribution and integration of cascaded couplers in the eight-layer stack of the 3G RSM module is under investigation, resulting in further advanced generation 4G of the RSM.

## Acknowledgment

Valuable contributions, recommendations and assistance during the manufacturing process and measurement from A. Schwarz (Cicor Microelectronics), J. Trabert, M. Huhn, M. Zocher and R. Stephan are highly appreciated.

Received: August 6, 2012.

## References

[1] D.R. Schroeder and L.J. Rexing, "LTCC multichip technology for military environments", Proceedings of the International Conference on Multichip Modules, pp. 612–617, April 1994.

[2] R.T. Knudson, E.J. Garcia, K.D. Patel, M. Okandan, C.K. Ho, C.D. James, S.B. Rohde, B.R. Rohrer, F. Smith, and L.R. Zawicki, "Low temperature co-fired ceramics in microelectronics, microsystems and sensors", 15th International Conference on Mixed Design of Integrated Circuits and Systems, MIXDES, pp. 23–37, June 2008.

[3] Leszek J. Golonka, Tomasz Zawada, Jacek Radojewski, Henryk Roguszczak, and Marcin Stefanow, "LTCC microfluidic system", International Journal of Applied Ceramic Technology, pp. 150–156, 2006.

[4] Ke Li Wu and Yong Huang, "LTCC technology and its applications in high frequency front-end modules", Proceeding of the 6th International Symposium on Antennas, Propagation and EM Theory, pp. 730–734, November 2003.

[5] S. Humbla, Jens Müller, Ralf Stephan, Dirk Stöpel, Johannes F. Trabert, Gabor Vogt, and Matthias A. Hein, "Reconfigurable Ka-band switch matrix for on-orbit verification", European Microwave Conference (EuMC), pp. 610–613, October 2009.

[6] T. Baras, S. Brosius, and A.F. Jacob, "K-band/S-band satellite transponder system for on-orbit evaluation of LTCC technology", European Radar Conference (EuRAD), pp. 348–351, October 2008.

[7] [Online] Homepage of the KERAMIS consortium. http://www.keramis.org

[8] S. Kaleem, J. Müller, S. Rentsch, R. Stephan, D. Stöpel, J.F. Trabert, G. Vogt, and M.A. Hein, "On-orbit verification of a 4 × 4 switch matrix for space applications based on the low temperature co-fired ceramics technology", 7th German Microwave Conference (GeMic), pp. 1–4, March 2012.

[9] [Online] "German TET-1 small satellite launched". http://www.dlr.de/dlr/en/desktopdefault.aspx/tabid-10261/371_read-4318/

[10] V. Siegfried, "The German Heinrich Hertz satellite mission", Proceedings of the 4th European Conference on Antennas and Propagation (EuCAP), pp. 1–4, April 2010.

[11] J. Trabert and M. Hein, "Impedance controlled coplanar waveguide system for the three dimensional distribution of high-bandwidth signals", Canadian Intellectual Property CA 2689154 A1, International Veröffentlichungsnummer WO 2008/155340 A1, December 2008.

[12] Giovanni Ghione and Carlo U. Naldi, "Coplanar waveguides for MMIC applications: effect of upper shielding, conductor backing, finite-extent ground planes and line-to-line coupling", IEEE Transactions on Microwave Theory and Techniques, vol. MTT-35, no. 3, pp. 260–267, March 1987.

[13] J.F. Trabert, K.H. Drüe, J. Müller, R. Stephan, and M.A. Hein, "High performance 3-dimensional hybrid-integrated switch matrix for Ka-band satellite communication applications based on ceramic multilayer technology", International Symposium on Microelectronics (IMAPS), November 2007.

[14] Chih-Chun Tsai, Yung-Shou Cheng, Ting-Yi Huang, and Ruey-Beei Wu, "A wide-band microstrip-to-microstrip multi-layered via transition using LTCC technology", Electrical Design of Advanced Packaging and Systems Symposium, December 2009.

[15] E.R. Pillai, "Coax via-A technique to reduce crosstalk and enhance impedance match at vias in high-frequency multilayer packages verified by FDTD and MoM modeling", IEEE Transaction on Microwave Theory and Techniques, vol. 45, no. 10, pp. 1981–1985, October 1997.

[16] P. Jeroma and G. Martin, "Moving reference planes for on-wafer measurements using the TRL calibration technique", 32nd Automatic RF Technique Group Conference (ARFTG), pp. 131–140, December 1988.

[17] Jeffrey A. Jargon and Roger B. Marks, "Two-tier multiline TRL for calibration of low-cost network analyzers", 46th Automatic RF Technique Group Conference (ARFTG), vol. 28, pp. 1–8, November 1995.

[18] S. Kaleem, S. Humbla, S. Rentsch, J. Trabert, D. Stöpel, J. Müller, and M.A. Hein, "Compact Ka-band reconfigurable switch matrix with power failure redundancy", 7th German Microwave Conference (GeMiC), pp. 1–4, March 2012.

[19] G. Radosavljevic, A. Maric, L. Zivanov, and W. Smetana, "Realization of high quality RF inductors using LTCC technology", 19th Telecommunication Forum (TELFOR), pp. 984–987, November 2011.

[20] R. Levy, "Explicit formulas for Chebychev impedance matching networks, filters and inter-stages", Proceedings

of the Institution of Electrical Engineers, vol. 111, issue 6, pp. 1099–1106, June 1964.
[21] Dale E. Dawson, "Closed form solutions for the design of optimum matching networks", IEEE Transaction on Microwave Theory and Techniques, vol. 57, no. 1, January 2009.
[22] R.L. Pease, A.H. Johnston, and J.L. Azarewicz, "Radiation testing of semiconductor devices for space electronics", Proceeding of the IEEE Conference, vol. 76, no. 11, pp. 1510–1526, November 1988.
[23] S. Humbla, K.H. Drüe, R. Stephan, D. Stöpel, J.F. Trabert, G. Vogt and M.A. Hein, "Qualification of a compact Ka-band switch matrix for on-orbit verification", German Microwave Conference (GeMiC), pp. 454–457, March 2008.
[24] H. Mextorf, T. Lehmann, and R. Knöchel, "Compact cascaded directional couplers with continuously tuneable coupling ratios", German Microwave Conference (GeMiC), pp. 1–4, March 2011.
[25] Masahiro Muraguchi, Takeshi Yukitake, and Yoshiyuki Naito, "Optimum design of 3-dB branch-line couplers using microstrip lines", IEEE MTT-S International Microwave Symposium Digest, vol. 31, August 1983, pp. 674–678.
[26] F. Hassam and S. Boumaiza, "Microstrip line based compact wideband branch-line coupler – lumped distributed element transformation", Canadian Conference on Electrical and Computer Engineering (CCECE), pp. 001007–001010, May 2008.